Journal of Magnetics 16(2), 114-119 (2011) DOI: 10.4283/JMAG.2011.16.2.114

Identification of Unknown Remanent Magnetization in the Ferromagnetic Ship Hull Utilizing Material Sensitivity Information Combined with Magnetization Modeling

Nam-Kyung Kim[1], Giwoo Jeung[1], Chang-Seob Yang[2], Hyun-Ju Chung[2], and Dong-Hun Kim[1]*

[1]Department of Electrical Engineering, Kyungpook University, Daegu 702-701, Korea
[2]The 6th R&D Institute-2, Agency for Defense Development, Changwon 645-600, Korea

(Received 24 March 2011, Received in final form 22 May 2011, Accepted 25 May 2011)

This paper presents a magnetization modeling method combined with material sensitivity information to identify the unknown magnetization distribution of a hull and improve the accuracy of the predicted fields. First, based on the magnetization modeling, the hull surface was divided into three-dimensional sheet elements, where the individual remanent magnetization was assumed to be constant. For a fast search of the optimum magnetization distribution on the hull, a material sensitivity formula containing the first-order gradient information of an objective function was combined with the magnetization modeling method. The feature of the proposed method is that it can provide a stable and accurate field solution, even in the vicinity of the hull. Finally, the validity of the method was tested using a scale model ship.

Keywords : adjoint variable method, inverse problems, Lagrange multiplier, magnetic anomaly, magnetization modeling

1. Introduction

Most ship hulls are constructed with ferromagnetic materials. When a ship is placed in the earth's magnetic field, steady-state magnetic signatures are created around the hull. This magnetic anomaly depends on the hull's magnetization, which can be classified as induced and remanent magnetization [1-6]. The calculus of the induced magnetization is easy to compute [1, 2]. On the other hand, the remanent magnetization depends on the magnetic history, such as mechanical and thermal stresses, etc. Normally, it is difficult to predict the field disturbance due to the remanent magnetization accurately because there is no information on such history. To date, a few attempts based on the Tikhonov's regularization have been made [1-3] but the method requires a very careful choice of the regularization parameter and also takes considerable computation time particularly for three-dimensional (3D) inverse problems.

To tackle the above defects, the authors proposed material sensitivity analysis in conjunction with magnetic dipole array modeling (MDM) in previous work [6], where the dipole array equivalent to the remanent magnetization on the hull was examined. Although its numerical implementation is relatively easy, an undesirable oscillation occurs in the predicted field values as an observation point approaches the array. Moreover, this method does not indicate the actual magnetization distribution in the hull, which could be very useful for demagnetizing the hull.

This paper presents a more elaborate method to calculate the underwater field anomaly around a ship by utilizing material sensitivity information to identify the unknown magnetization distribution of a hull and improve the accuracy of the predicted fields. First, based on the magnetization modeling method (MMM), the hull surface was divided into 3D sheet elements where individual remanent magnetization was assumed to be constant. For a fast search of the optimum magnetization distribution on the hull, a material sensitivity formula containing first-order gradient information of an objective function was combined with the MMM [4-8]. For numerical implementation, a general optimizer, called DOT in [9], was adopted to guarantee the convergence of the objective function. The feature of the method is that it can provide a stable and accurate field solution, even in the vicinity of the hull.

Finally, the validity of the proposed methods was tested with a scale model ship and field signals predicted from

*Corresponding author: Tel: +82-53-950-5603
Fax: +82-53-950-5603, e-mail: dh29kim@ee.knu.ac.kr

the two methods, MDM and MMM, were investigated thoroughly with reference to experimental data.

2. Magnetization Modeling

The MDM and MMM differ by how they model the ship hull. In both methods, the unknowns are the magnetization, which has three-directional components in a rectangular coordinate system. In the case of the MDM, the hull's magnetization is replaced with the equivalent magnetic dipole array shown in Fig. 1(a), where each circle denotes a magnetic dipole. The underwater magnetic anomaly due to the remanent magnetization of the hull is then calculated from the equivalent dipole array obtained after solving an inverse problem. On the other hand, the MMM requires sheet elements forming the hull surface where equivalently constant magnetic moment vectors are sought, as shown in Fig. 1(b). When the hull thickness is relatively small and the permeability is high, the magnetic moment can be assumed to be parallel to the hull surface [1].

Consider a ferromagnetic ship hull placed in the earth's magnetic field $\mathbf{H}_o$. A local perturbation of the field $\mathbf{H}_{red}$ expressed in terms of the magnetic reduced potential ϕ_m is created around the ship.

$$\mathbf{H}=\mathbf{H}_o+\mathbf{H}_{red}=\mathbf{H}_o-\nabla\phi_m \tag{1}$$

The field $\mathbf{H}_{red}$ is due to the hull magnetization $\mathbf{M}$ equal to the sum of the induced magnetization $\mathbf{M}_{ind}$ and the remanent one $\mathbf{M}_{rem}$.

$$\mathbf{M}=\mathbf{M}_{ind}+\mathbf{M}_{rem} \tag{2}$$

This paper focused only the field anomaly due to remanent magnetization. This is because the field perturbation of the induced magnetization can be calculated easily [1, 2]. If the optimum moment values in a dipole array or on the sheet elements of the hull are decided, the field perturbation $\mathbf{H}_{red}$ due to the remanent magnetization $\mathbf{M}_{rem}$ can be calculated using the following equation [1, 2].

$$\begin{aligned}\mathbf{H}_{red}&=\frac{1}{4\pi}\int_V\frac{3(\mathbf{M}_{rem}-\mathbf{r})\mathbf{r}-r^2\mathbf{M}_{rem}}{r^5}dV\\&=-\frac{1}{4\pi}\int_S\mathbf{M}_{rem}\cdot\mathbf{n}\frac{r}{r^3}dS\end{aligned} \tag{3}$$

where V is the volume enclosing the magnetization $\mathbf{M}_{rem}$, S is the sheet element, $\mathbf{n}$ is the unit vector normal to the surface of V or the edge of S, and $\mathbf{r}$ means the displacement vector from the magnetic moment to the observation point.

3. Material Sensitivity Information

By exploiting the adjoint variable method and augmented objective function, a material sensitivity formula with respect to the equivalent magnetic moment of the hull, was derived analytically [4-7]. Consider an objective function F defined in the analysis domain of interest Ω for magnetostatic inverse systems,

$$F=\int_\Omega g(\mathbf{B}(\mathbf{p}))d\Omega \tag{4}$$

where g is a scalar function differentiable with respect to the magnetic flux density $\mathbf{B}(\mathbf{p})$, which is itself an implicit function of the system parameter $\mathbf{p}$. To deduce a material sensitivity formula, and adjoint system equation systematically, the variational of equation (5), which is referred to as the primary system, was added to equation (4).

$$\nabla\times(\nu\nabla\times\mathbf{A}-\mathbf{M}_{rem})=0 \tag{5}$$

where n is the magnetic reluctivity and $\mathbf{A}$ is the magnetic vector potential. Exploiting the augmented Lagrangian method and first vector Green's theorem, the sum of the two equations can be written as:

$$\begin{aligned}\bar{F}&=\int_\Omega g d\Omega+\int_\Omega\lambda[-\nabla\times(\nu_o\nabla\times\mathbf{A}-\mathbf{M}_{rem})]d\Omega\\&=\int_\Omega g d\Omega-\int_\Omega\nu_o(\nabla\times\mathbf{A})\cdot(\nabla\times\lambda)d\Omega\\&\quad+\int_\Omega\mathbf{M}_{rem}\cdot(\nabla\times\lambda)d\Omega\end{aligned} \tag{6}$$

where λ is the Lagrange multiplier vector interpreted as the adjoint variable.

By taking the variation of both sides of equation (6) with respect to a small change δp in the system parameter, the first variation of the augmented objective function $\delta\bar{F}$ can be developed as follows:

$$\begin{aligned}\delta\bar{F}=&-\int_\Omega\left[\mathbf{g}\cdot\nabla\times\left(\delta\mathbf{A}+\frac{\partial\mathbf{A}}{\partial\mathbf{p}}\delta\mathbf{p}\right)\right]d\Omega\\&-\int_\Omega\left[\nu_o\left(\nabla\times\left(\delta\mathbf{A}+\frac{\partial\mathbf{A}}{\partial\mathbf{p}}\delta\mathbf{p}\right)\right)\cdot(\nabla\times\lambda)\right.\\&\left.+\nu_o(\nabla\times\mathbf{A})\cdot\left(\nabla\times\left(\delta\lambda+\frac{\partial\lambda}{\partial\mathbf{p}}\delta\mathbf{p}\right)\right)\right]d\Omega\\&+\int_\Omega\left[\frac{\partial\mathbf{M}_{rem}}{\partial\mathbf{p}}\delta\mathbf{p}\cdot(\nabla\times\lambda)+\mathbf{M}_{rem}\cdot\left(\nabla\times\left(\delta\lambda+\frac{\partial\lambda}{\partial\mathbf{p}}\delta\mathbf{p}\right)\right)\right]d\Omega\end{aligned} \tag{7}$$

where $\mathbf{g}\equiv\partial g/\partial(\nabla\times\mathbf{A})$ corresponds to the pseudo-source of the adjoint system. For the simplicity of equation (7), the arbitrary variables, $(\delta\mathbf{A}+(\partial\mathbf{A}/\partial\mathbf{p})\delta\mathbf{p})$ and $(\delta\lambda+(\partial\lambda/\partial\mathbf{p})\delta\mathbf{p})$, can be replaced by an alternative notation, e.g. $\bar{\lambda}$ and $\bar{\mathbf{A}}$, respectively. The sum of the two integrands, including the term $\bar{\mathbf{A}}$ on the right-hand side of equation (7), becomes

zero because it is identical to the variational form of the primary system. The terms relevant to $\bar{\lambda}$ were also set to zero as follows:

$$\int_\Omega \nu_o(\nabla \times \bar{\lambda}) \cdot (\nabla \times \lambda) d\Omega + \int_\Omega \mathbf{g} \cdot \nabla \times \bar{\lambda} d\Omega = 0 \qquad (8)$$

Equation (8) is the variational of the adjoint system and the pseudo-source vector, **g**, induced by the partial differential of the objective function. Overall, the pseudo-source plays the role of the magnetic source, i.e., equivalent magnetization in the adjoint system.

Deleting all the terms involving $\bar{\lambda}$ and $\bar{\mathbf{A}}$ from equation (7), a material sensitivity formula applicable to magnetostatic inverse problems can be derived as:

$$\frac{dF}{dp} = \int_\Omega \frac{\partial \mathbf{M}_{rem}}{\partial \mathbf{p}} \cdot (\nabla \times \lambda) d\Omega \qquad (9)$$

where λ is the solution of the adjoint system equation (8), i.e., the counterpart of solution **A** of the primary system equation (5).

4. Numerical Implementation

To simplify the numerical implementation, the magnetic moment $\mathbf{M}_{rem}$ was forced to be a linear function of the system parameter **p** [7]. A general-purpose optimization control program, DOT, based on the Broydon-Fletcher-Goldfarb-Shanno (BFGS) algorithm in [9] was adopted to accelerate the convergence of the objective function. The optimum magnetization values corresponding to the center points of all sheet elements shown in Fig. 1(b) were determined, and all values were initially set to zero. Under the

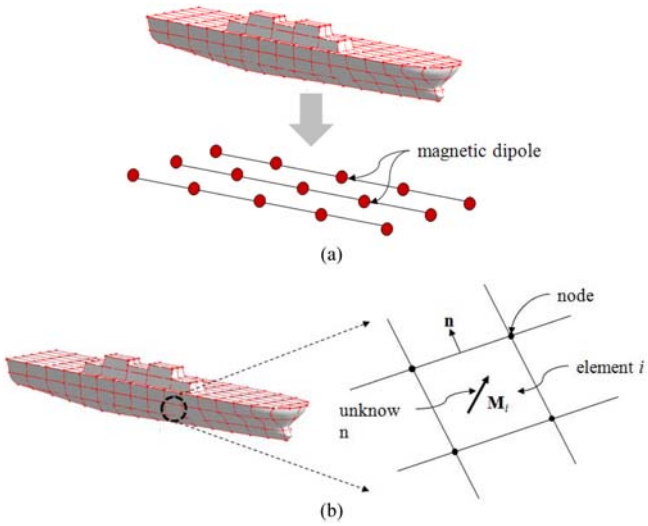

Fig. 1. Two modeling methods of a hull's magnetization: (a) magnetic dipole array of MDM, (b) equivalent magnetic moment of MMM.

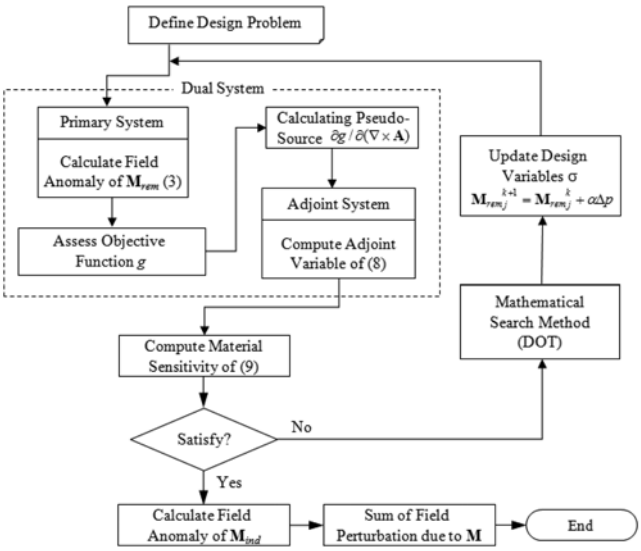

Fig. 2. Flowchart of the proposed program architecture for solving an inverse problem.

proposed program architecture, the iterative design process in Fig. 2 involves the following steps:

Step 1: Define an objective function with the target field data.

Step 2: Calculate the field perturbation due to the remanent magnetization of the hull with equation (3) at the selected observation points.

Step 3: Assess the objective function and calculate the adjoint source at the observation points.

Step 4: Compute the adjoint variable λ from equation (8) and the sensitivity value at each magnetization moment with equation (9).

Step 5: Update magnetization moment values $\mathbf{M}_{rem}$ ($\mathbf{M}_{rem\,j}^{k+1} = \mathbf{M}_{rem\,j}^{k} + \alpha \Delta p$) at the *k*th iteration, where *j* and α are the *j*th sheet element and relaxation factor, respectively.

Step 6: Check convergence and go to step 2 if unsatisfactory.

Step 7: Calculate the field anomaly of $\mathbf{M}_{ind}$ and sum up the total field perturbation due to **M** of equation (1).

5. Experiments and Results

5.1. Experimental setup

To validate the proposed method, a scale model ship in Fig. 3 made out of steel plate with an upper deck thickness, lower deck thickness and relative permeability of 0.3 mm, 0.6 mm and 160, respectively, was considered. The dimensions of the mock-up were 2.4 m long, 0.5 m wide and 0.25 m high. The magnetic signature generated

Fig. 3. A photograph of a scale model ship.

by the hull under the earth's magnetic field was measured with four tri-axial magnetic sensors located under the keel line of the ship, as shown in Fig. 4. Instead of using many sensors, the experiment was carried out as the ship slowly moves along the x axis heading for the North Magnetic Pole against the sensor at a standstill. The x and z components of the earth's magnetic field at an experimental station are 307 mG and 377 mG, respectively. The field components due to the remanent magnetization were taken by subtracting the induction field due to the induced magnetization from the measured data. For this process, the induced field was calculated using a commercial EM software package, MagNet 6 [10].

5.2. Comparison of predicted fields

To predict the field anomaly due to the magnetization distributed over the ferromagnetic hull, the hull surface shown in Fig. 1 was divided into 322 sheet elements, where the optimum magnetization distribution was calculated. The objective function was defined at a reference depth of 1 m under the keel line depicted in Fig. 4.

$$F = \sum_{i=1}^{n} \sum_{j=1}^{3} (B_{ij}^{k} - B_{oij})^2 \tag{10}$$

where n is the total observation points of 101, B_{ij}^{k} is the jth component of the magnetic flux density predicted at the ith observation point for the kth iterative design stage and B_{oij} is the target fields measured at the observation points.

According to the flowchart in Fig. 2, the total field anomaly due to the hull's magnetization, $\mathbf{M}_{ind}$ and $\mathbf{M}_{rem}$, are computed along three different depths of 0.5 m, 1 m and 4 m. After solving the inverse problem, the optimum magnetization distribution over the hull is illustrated in Fig. 5, where the direction and magnitude of the magneti-

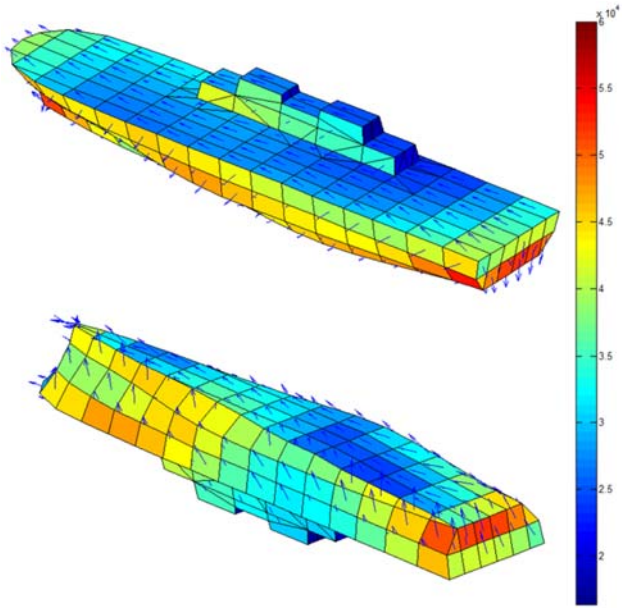

Fig. 5. Optimum magnetization distribution after solving the inverse problem.

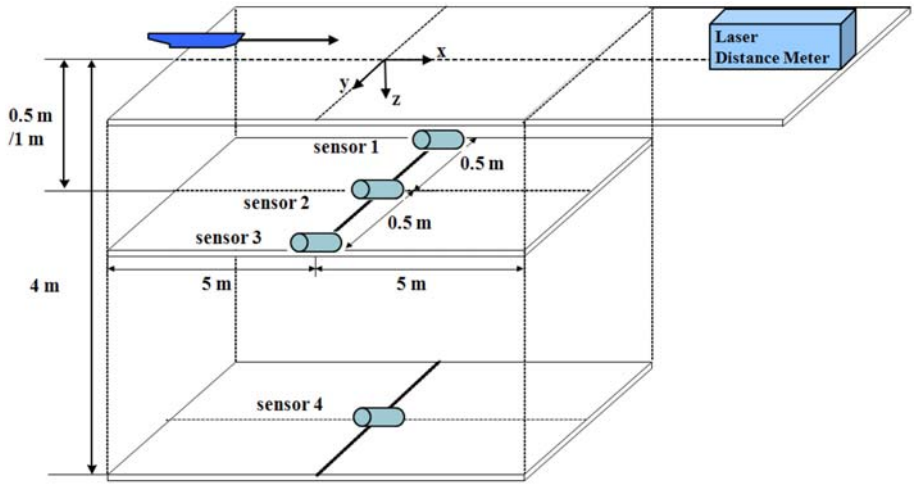

Fig. 4. Experimental setup.

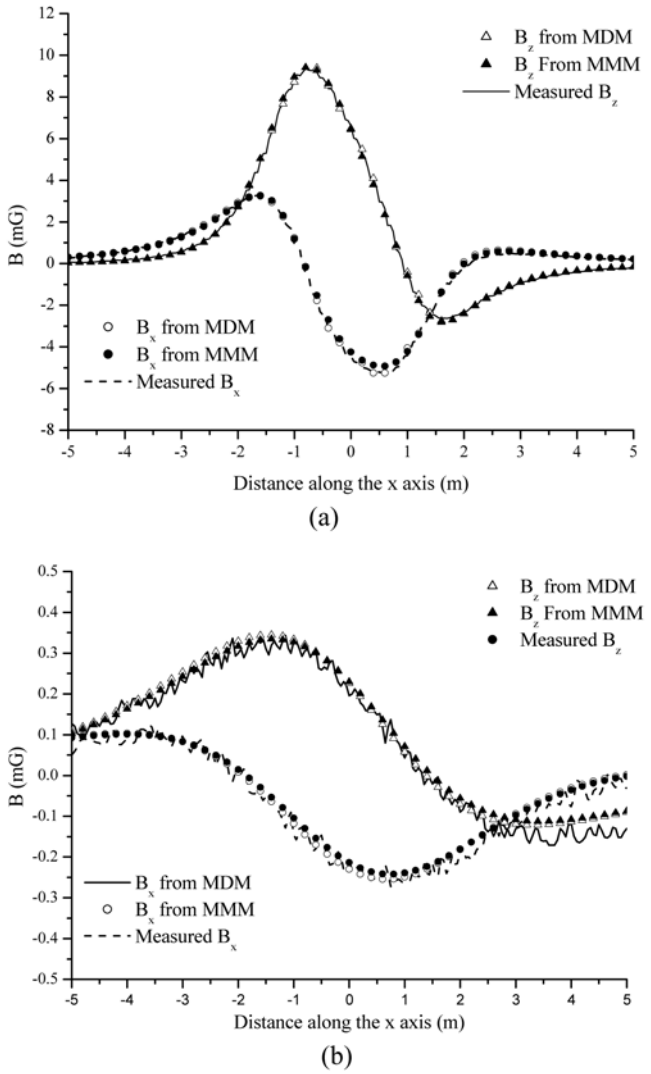

Fig. 6. Comparison of the field anomaly predicted by two different methods, MDM and MCM, with the measured field at different depths away from the keel line: (a) 1 m in depth, (b) 4 m in depth.

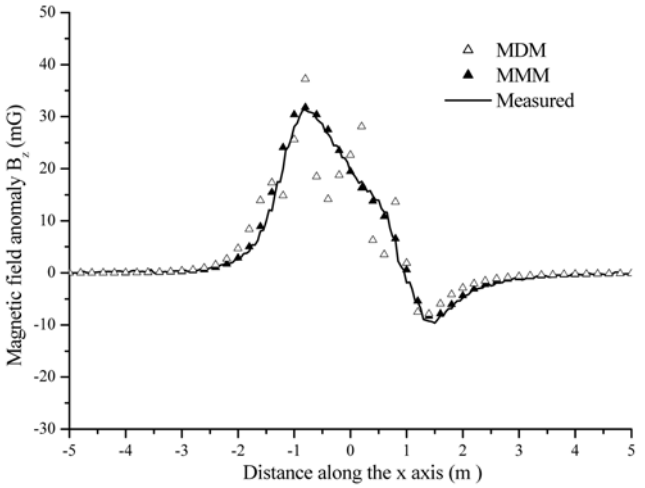

Fig. 7. Comparison of the field anomaly predicted by two different methods, MDM and MCM, with the measured field at 0.5 m under the keel line.

Table 1. Comparison of the two different methods for predicting the field anomaly due to a ferromagnetic hull.

Component	MDM	MMM
Unknown	magnetic dipole	magnetization moment
Number of unknowns	45	966
Ship modeling technique	easy (2D)	relatively hard (3D)
Computing time	28 sec.	37 sec.
Field error in |**B**| in depth		
0.5 m	125%	8.47%
1 m	0.73%	0.51%
4 m	6.18%	3.05%

Normalized field error was computed by $|Pred\text{-}Meas|/Meas$ where *Pred* stands for predicted field and *Meas* is the measured field.

zation vector is expressed in terms of arrows and color contours.

Fig. 6 shows a comparison of the predicted and measured fields at the depths of 1 m and 4 m apart from the keel line. The predicted fields in Fig. 6(b) were calculated by exploiting the optimum magnetization distribution obtained in Fig. 4. The results showed that the MMM and MDM had good agreement with the measured data. The accuracy of the methods is also examined near the bottom of the ship. Fig. 7 compares the predicted fields with the experimental data at a depth of 0.5 m. The MDM includes relatively large errors in the field solutions compared to the MMM. In particular, in the case of the MDM, an undesirable numerical oscillation occurs in the predicted fields. The oscillation comes from the small number of the magnetic dipoles used for the field prediction.

The features of the two methods for predicting the underwater field anomaly around the ship due to the ferromagnetic hull were compared with each other in Table 1. The proposed method produced a stable and reliable field solution, even in the vicinity of the waterline of the ship compared to the MDM.

6. Conclusion

This paper presents a more accurate methodology for predicting the underwater field anomaly around the ship. The optimum magnetization distribution on the hull was determined successfully based on the magnetization modeling method combined with the material sensitivity information. The results show that the proposed method can provide a stable and accurate field solution, even in the

vicinity of the hull compared to the magnetic dipole array method.

Acknowledgment

This work has been supported by the Low Observable Technology Research Center program of Defense Acquisition Program Administration and Agency for Defense Development.

References

[1] O. Chadebec, J.-L. Coulomb, J.-P. Bongiraud, G. Cauffet, and P. Le Thiec, IEEE Trans. Magn. **38**, 1005 (2002).
[2] O. Chadebec, J.-L. Coulomb, G. Cauffet, and J.-P. Bongiraud, IEEE Trans. Magn. **39**, 1634 (2004).
[3] Y. Vuillerment, O. Chadebec, J.-L. Coulomb, L. Rouve, G. Cauffet, J.-P. Bongiraud, and L. Demilier, IEEE Trans. Magn. **44**, 1054 (2008).
[4] C. Yang, K. Lee, G. Jung, H. Chung, J. Park, and D. Kim, J. Appl. Phys. **103**, 905 (2008).
[5] K. Lee, G. Jung, C. Yang, H. Chung, J. Park, H. Kim, and D. Kim, IEEE Trans. Magn. **45**, 1478 (2009).
[6] G. Jung, C. Yang, H. Chung, S. Lee, and D. Kim, IEEE Trans. Magn. **45**, 4169 (2009).
[7] D. Kim, K. Ship, and J. Sykulski, IEEE Trans. Magn. **40**, 1156 (2004).
[8] D. Kim, J. Sykulski, and D. Lowther, IEEE Trans. Magn. **41**, 1752 (2005).
[9] DOT User Manual, Vanderplaats Research & Development, Inc., Springs, Colorado (2001) pp. 30~71.
[10] MagNet 6 User's Guide, Infolytica Corporation, Quebec (2005) pp. 78~100.